Hindawi
Advances in Polymer Technology
Volume 2023, Article ID 6612220, 10 pages
https://doi.org/10.1155/2023/6612220

Research Article

Preparation of Chiral Epoxy Resins and the Optically Active Cured Products

Xinyuan Tang, Ming Hu, Xiaoran Liu, Yanyun Li, Junying Zhang, and Jue Cheng

Key Laboratory of Carbon Fiber and Functional Polymers, Ministry of Education, Beijing University of Chemical Technology, Beijing 100029, China

Correspondence should be addressed to Junying Zhang; zhangjy@mail.buct.edu.cn and Jue Cheng; chengjue@mail.buct.edu.cn

Received 7 August 2023; Revised 10 September 2023; Accepted 21 September 2023; Published 14 October 2023

Academic Editor: Wen Li

Chirality is one of the most common and significant phenomenon in nature, and epoxy resin is one of the most widely used and researched thermosetting resins, however the influences of chiral carbon in epoxy group on the performances of the cured epoxy resins have ever been hardly studied, therefore it is crucial and meaningful to explore the structure–function relationship of chirality and performance of epoxy resins. Herein, from the analysis of synthesis mechanism, the different chiral configuration with high percent enantiomeric excess (>99%) and racemic bisphenol A epoxy resins were simply prepared by controlling the chirality of epichlorohydrin. The apparent activation energy of the curing process with D230 was calculated by Kissinger method and Flynn–Wall–Ozawa method, respectively, and both results indicate that chirality have no effect on the curing reaction. We found that the secondary structure of epoxy monomer is untouched by its chirality, and they are all right helix structure. For this reason, the thermal stability, glass transition temperature, and thermomechanical properties of diverse chiral epoxy resins cured by D230 have no significant difference. Nevertheless, it was found that the optical rotation activity of chiral epoxy resins can be partially maintained after curing reaction, it manifests the cured products of chiral epoxy resins possesses the possibility of application in the field of polarized materials.

1. Introduction

Chirality is a fundamental symmetry property in nature. It is present at several scales going from elementary particles even to astronomical objects, and it has important applications in chemistry, biology, physics, pharmacy and other fields [1–3]. From this point of view, the synthesis of optically active polymers has attracted attention of materials scientists [4]. Therefore, a scenario of hierarchical chirality spanning from elemental particles to atoms, molecules, supramolecules, polymers, and supramolecular polymers has been extensively researched [5–8]. To elucidate, a majority of researches in oligomers [9, 10], σ-conjugated polymers [11–13], and π-conjugated polymers [14–16] have been widely studied until now. However, few studies have investigated whether different chiral configurations have any effect on the performance of cross-linked polymerization systems like epoxy resins.

Epoxy is one of the most extensively used conventional thermosetting polymers [17–20], and it has been widely employed in numerous industrial applications such as adhesives [21–23], electronic devices [24–26], encapsulations [27], coatings [28–30], marine systems [31, 32], and aerospace [33] parts owing to its high-tensile strength and Young's modulus, and excellent adhesion, thermal stability, solvent resistance, thermal insulation, chemical resistance, and dielectric properties. Moreover, chiral carbon is always present in the epoxy group in most common epoxides, as shown in Scheme 1. Therefore, it is highly urgent to investigate whether the different chiral carbon configurations have impact on the properties of epoxy resins.

Nevertheless, in the field of epoxy resins, how to synthesize chiral epoxy resins has hardly been studied. Although there are many methods to synthesize chiral epoxides, for instance, Sharpless asymmetric epoxidation [34–37], Jacobsen's asymmetric epoxidation [38, 39], and biological ways [40–43] using biocatalysts such as enzymes and recombinant cells, these preparation methods are expensive and involve complicated steps that are not suitable for large-scale preparation and testing of polymer materials. Moreover, we proposed that by controlling the single configuration of epichlorohydrin

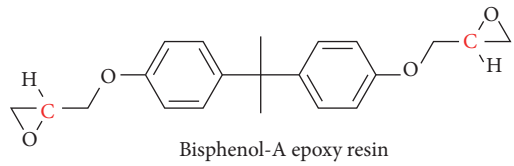

Bisphenol-A epoxy resin

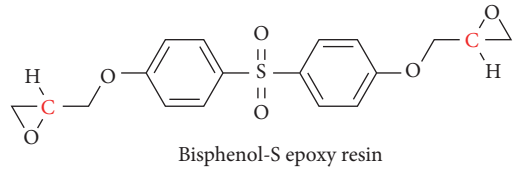

Bisphenol-S epoxy resin

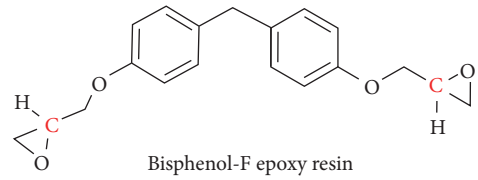

Bisphenol-F epoxy resin

Scheme 1: Common bisphenol-based epoxy resins.

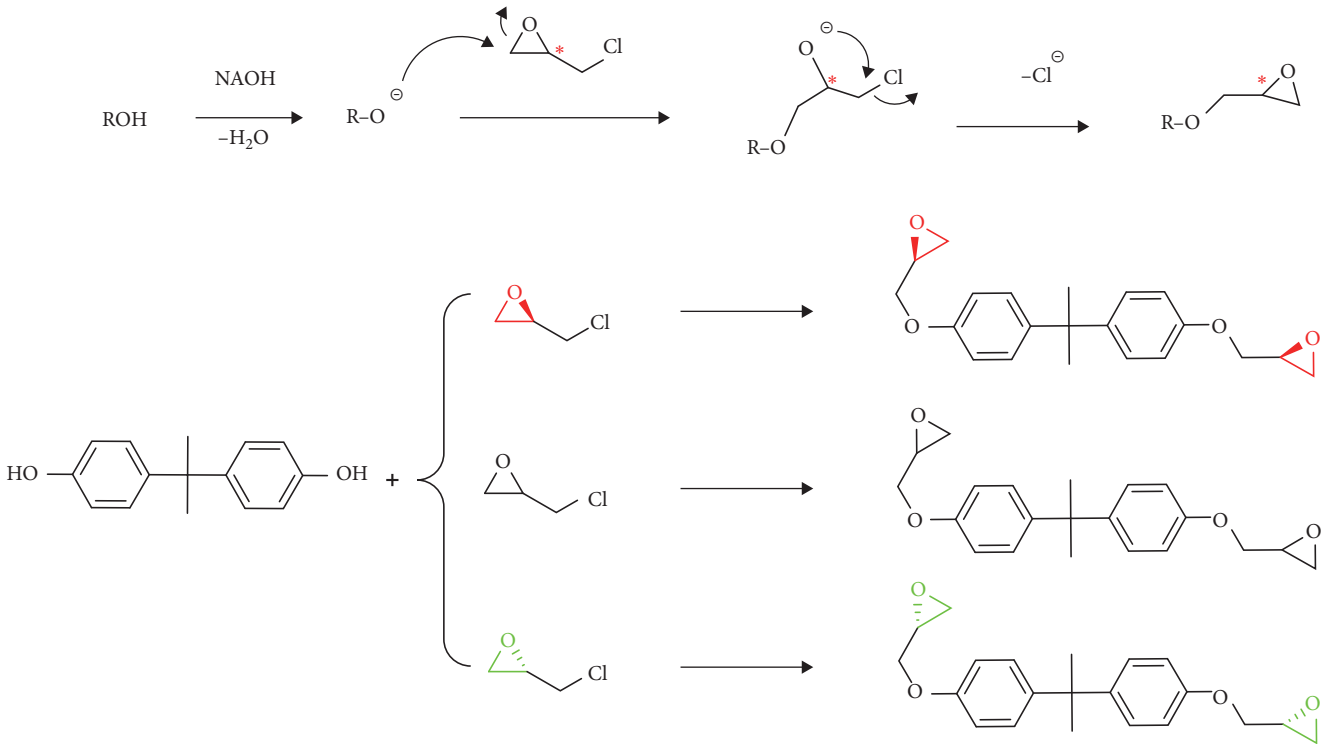

Scheme 2: Mechanism and reactions of epoxy resin synthesis.

(ECH), large-scale preparation of chiral epoxy resins can be simply achieved in one-pot reaction through analysis the synthetic mechanism of epoxy resin by epichlorohydrin method, as shown in Scheme 2. We realized that, during the reaction, the epoxy group undergoes a ring-opening and then a ring-closing reaction under the action of the oxygen anion. However, throughout the entire process, the chiral carbon atoms do not experience any breaking of covalent bonds. This means that the chiral configuration of the carbon atoms will be maintained in the entire reaction, so we can control the chiral configuration of the resulting epoxy resin by controlling the chiral carbon configuration of ECH, as one of the raw materials.

In this study, we synthesized racemic bisphenol A epoxy resin (DGEBA), (R, R)-bisphenol A epoxy resin (R-DGEBA), and (S, S)-bisphenol A epoxy resin (S-DGEBA), respectively, by controlling the stereoconfiguration of the ECH. This method is suitable for all epoxides synthesized by ECH

method. By curing the three epoxy resins using polyether amine (D230), we calculated the activation energies (E_a) of the three curing systems separately and characterized the fundamental properties of the three cross-linked polymer systems in exploring the chiral configuration would affect, which performance of the cross-linked epoxy resins.

2. Experimental Section

2.1. Materials. Bisphenol A, ECH, (R)-epichlorohydrin, (S)-epichlorohydrin, tetrabutylammonium bromide (TMAB), acetonitrile, and polyether amine D230 were purchased from Macklin-reagent Co., China. Sodium hydroxide, distilled water, and anhydrous sodium sulfate were obtained from Sinopharm Chemical Reagent Co., Ltd. All reagents used are analytically pure and used directly after purchase without further treatment.

2.2. Characterizations. ^{1}H NMR and ^{13}C NMR spectra were recorded by an AVANCE III Bruker NMR spectrometer (Bruker, Switzerland) with $CDCl_3$ as solvents, operating at 400 MHz. Mass spectrometry test is performed on a mass spectrometry analyzer (Model: Agilent Technologies 6540 UHD) with the positive ion mode selected, using acetonitrile as solvent. FTIR spectra were measured on a Bruker Alpha FTIR at a resolution of 4 cm^{-1} in the wavenumber range of 4,000–400 cm^{-1} using KBr pellets. The optical material current WZZ-2B gyroscope was used for the rotatory test and the test light source was sodium D light lamp, and the detection wavelength was 589 nm^{-1}. Circular dichroism (CD) and ultraviolet (UV–Vis) absorption spectroscopy measurements were conducted on a Jasco 810 spectropolarimeter. Using JC-002 high-performance liquid chromatography (HPLC), the epoxy resins with different configurations were separated to characterize the enantiomer excess by Y4 column with the size of 250 × 4.6 mm, 5 μm, ethanol as solvent, and 10 μL was injected at 25°C at the flow rate of 1.0 mL min. The thermal stability was tested by thermogravimetric analysis (TGA) measurements, which were carried out on a TGA Q50 analyzer at a heating rate of 10°C min^{-1} in N_2 atmosphere (from 25 to 800°C). DMA was used to characterize the thermal mechanical properties by a TA Q800 instrument. Samples were tested with a film tensile mode at a heating rate of 5°C min^{-1} from −50 to 150°C: the oscillatory frequency was 1 Hz. Dielectric properties were tested with a precision impedance analyzer by an Agilent 4294A Instrument at 25°C and frequency scanning range is 10^4–10^7 Hz. The crystallinity was examined by wide-angle X-ray scattering (WAXS) measurements using a Rigaku D/Max 2,500 VB2+/PC diffractometer with Cu Ka radiation. The fractured morphology (broken in liquid nitrogen) was characterized by a JEOL JSM-6700M SEM at an accelerating voltage of 5 kV, and all the surfaces of the samples were coated with gold to improve the conductivity and prevent charging. Differential scanning calorimeter (DSC) tests were carried out on a TA Instruments Q20 equipped with an RCS 90 cooling system under N_2 atmosphere, and the cured epoxy resins were heated from 0 to 180°C at a heating rate of 10°C/min.

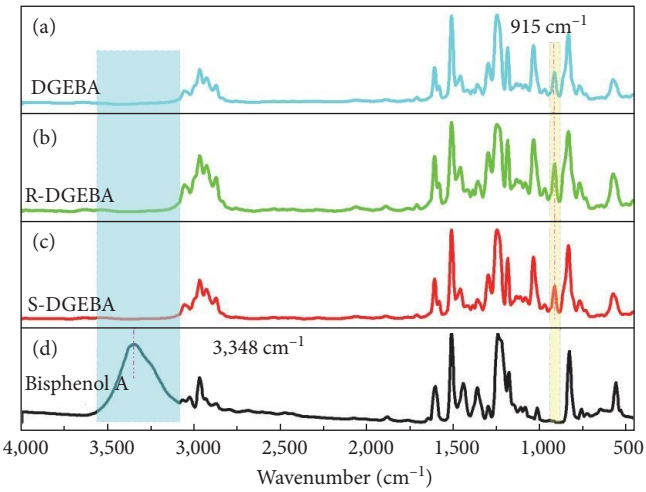

FIGURE 1: FTIR spectra of Bisphenol A, DGEBA, R-DGEBA, and S-DGEBA (a–d).

2.3. Synthesis of DGEBA, R-DGEBA, and S-DGEBA. Bisphenol A (50 g, 0.22 mol) and epichlorohydrin (405 g, 4.4 mol), (R)-epichlorohydrin, and (S)-epichlorohydrin were added, respectively, into a 500 mL four-necked flask, equipped with a condenser and a thermometer and stirred at room temperature for 0.5 hr until it is completely dissolved. Then, tetramethyl ammonium bromide (0.54 g, 2.4 mol%) was placed and the mixture was stirred at 65°C for 15 min. After that, solid sodium hydroxide (NaOH) (21 g, 0.525 mol) was added in six batches in 1 hr, and the mixture was stirred in nitrogen atmosphere. After that, the mixture was reacted at 65°C for 3 hr. Next, the excess sodium hydroxide and the salt produced by the reaction were removed by filtration and the mixed liquid were washed by hot distilled water for five times. Before removing the excess epichlorohydrin on a rotary evaporator, the liquid was dried with anhydrous sodium sulfate at room temperature for 12 hr and the transparent viscous products were obtained in last.

2.4. Preparation of the Cured Epoxy Resins. DGEBA, R-DGEBA, and S-DGEBA were cured with a commonly used curing agent D230. Epoxy monomers were mixed with D230 in a 1 : 1 equiv ratio. The mixture was cured in a blasting oven at 80°C for 2 hr, 120°C for 2 hr, and 140°C for 3 hr.

3. Results and Discussion

3.1. Synthesis and Characterization of DGEBA, R-DGEBA, and S-DGEBA. In this paper, bisphenol, NaOH, TMAB, and ECH in different chiral configuration were reacted in one pot, respectively. The epoxide groups in ECH are first opening by addition and then reformed by intramolecular substitution reaction. Finally, DGEBA, R-DGEBA, and S-DGEBA were obtained by controlling the chirality of ECH. The chemical structures of the synthesized monomers were confirmed by FTIR, MS, ^{1}H NMR, and ^{13}C NMR. Figure 1 presents the FTIR spectra of bisphenol A, DGEBA, R-DGEBA, and S-DGEBA.

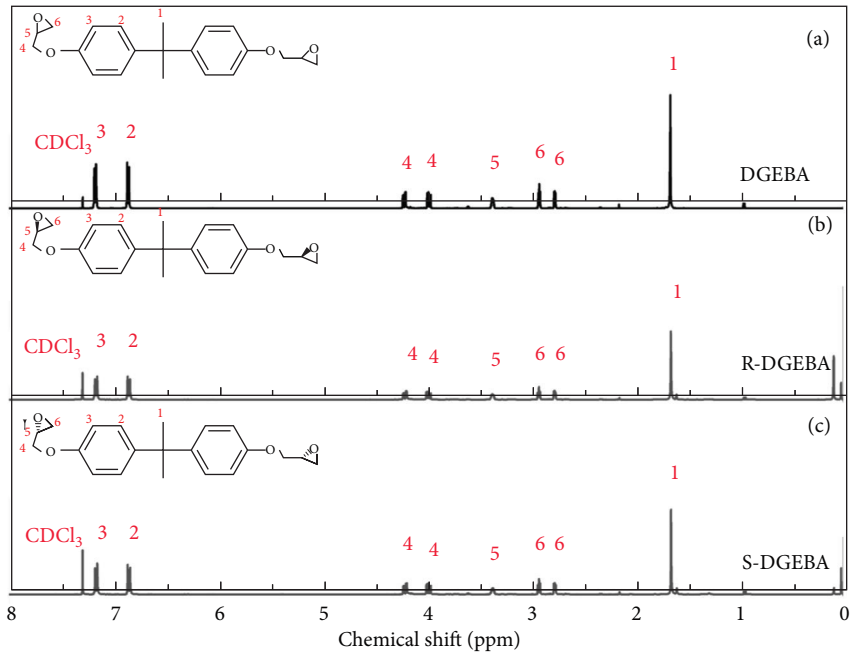

FIGURE 2: ^{1}H NMR of the (a) DGEBA, (b) R-DGEBA, and (c) S-DGEBA.

TABLE 1: Results from HPLC and polariscope measurements.

Samples	$\alpha_D{}^{20}$ (a)	ee (%)(b)
DGEBA	0°	–
R-DGEBA	14.3°	99.99
S-DGEBA	−14.1°	91.74

[a]Specific rotation measured at 20°C using sodium light lamp D. [b]Enantiomeric excess.

In the FTIR spectra of DGEBA, R-DGEBA, and S-DGEBA, the characteristic peak of O–H at around 3,348 cm^{-1} disappeared and the peak at around 915 cm^{-1} belonging to the epoxy group appeared. As shown in Figure 2(c) and Figure S1, the chemical shift in ^{1}H NMR and ^{13}C NMR spectra of the three kinds of epoxy resins have no difference, because NMR cannot detect the difference of chiral enantiomers [44, 45]. DGEBA, R-DGEBA, S-DGEBA: ^{1}H NMR (CDCl3): $\delta = 1.66$ (s, 6H, 1); 6.84 (m, 4H, 2); 7.15 (m, 4H, 3); 4.19 (dd, 2H, 4); 3.97 (dd, 2H, 4); 3.36 (m, 2H, 5); 2.76 (dd, 2H, 6); 2.91 ppm (dd, 2H, 6). ^{13}C NMR (CDCl3): $\delta = 27.97$ (CH_3, 1); 40.69 (C, 2); 142.61 (C, 3); 126.75 (CH, 4); 112.97 (CH, 5); 155.29 (C, 6); 67.71 (CH_2, 7); 49.16 (CH, 8); 43.76 ppm (CH_2, 9).

And the MS spectra is shown in Figure S2, the results of HPLC and polariscope are presented in Table 1.

In the Table 1, the specific optical rotations of DGEBA, R-DGEBA, S-DGEBA are 0°, 14.3°, −14.1°, respectively, and ee% values of both R-DGEBA and S-DGEBA are greater than 90%. These results indicate that the target epoxy resins in different chiral configuration were synthesized successfully including the racemic one (DGEBA) and the chiral two resins (R-DGEBA and S-DGEBA).

3.2. Curing Process. The nonisothermal curing kinetics of DGEBA-D230, R-DGEBA-D230, and S-DGEBA-D230 were studied by DSC. In each system, heating rates at 5, 10, 15, and 20°C/min are used, respectively. The Kissinger's method (Equation (1)) [46–48], and Flynn–Wall–Ozawa (FWO) method (Equation (2)) [49, 50] were used to obtain the apparent activation energy during the curing process.

$$\ln\left(\frac{\beta}{T_p^2}\right) = \ln\left(\frac{AR}{E_a}\right) - E_a/RT_p, \quad (1)$$

$$\ln\beta = \mathrm{Const}A - 1.052\,E_a/RT, \quad (2)$$

where β is the heating rate, T_p is the exothermic peak temperature, E_a is the activation energy, R is the gas constant, A is the pre-exponential factor. The results of DSC tests at different temperature rate and calculations of conversion versus temperature by FWO method are illustrated in Figure S3 and the data are summarized in Table S1. As shown in Figure 3, the E_a of the three kinds of curing system both on the two methods is basically same, and we believe the reason is that the D230 as curing agent is achiral and the curing reaction happens on the achiral carbon of epoxy group in the epoxy resins (Scheme 1), so the different chirality configuration of epoxy resins do not affect the parameters of curing reaction.

FTIR spectra of DGEBA, R-DGEBA, and S-DGEBA before and after curing are exhibited in Figure 4. Compared with the FTIR spectra before curing, the peaks for epoxy groups at around 914 cm^{-1} disappeared and broad peaks at around 3,500 cm^{-1} representing O–H from the ring-opening reaction between epoxy groups and amines appeared in the FTIR spectra after curing. This means that the epoxy systems were cured well under the former mentioned conditions.

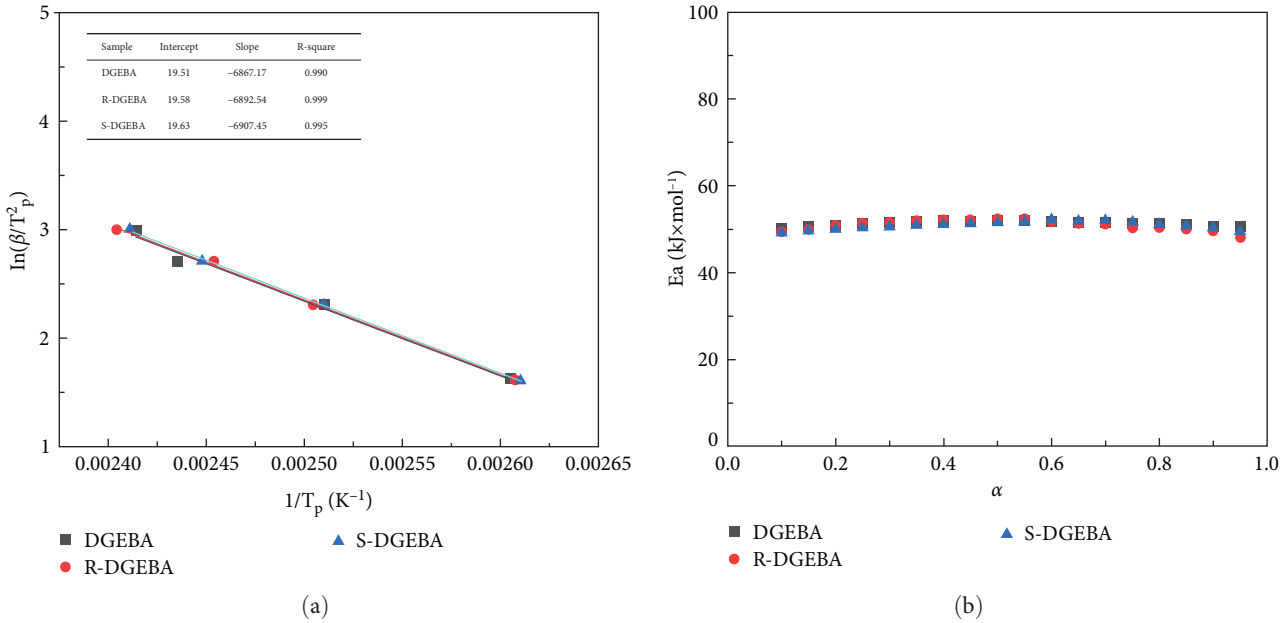

FIGURE 3: Linear plots of (a) $-\ln(\beta/T_p^2)$ versus $1/T_p$ based on Kissinger's equation and (b) E_a versus α (conversion rate) based on FWO theory.

3.3. Thermal Stability, Glass Transition Temperature, and Thermomechanical Properties. The TGA and DTG curves of the cured epoxy resins under N_2 are illustrated in Figure S4, and the data are summarized in Table S2. The glass transition temperature is measured by DSC and DMA, respectively, and the storage modulus and loss modulus are also determined by DMA, and the results are summarized in Figure S5 and Table S3. From all the data above, all the cured epoxy resins exhibit semblable thermal stability, glass transition temperature, and thermomechanical properties. This indicates the network framework of polymer does not change significantly with different chiral configurations of epoxy group. And the results of XRD diagram (Figure S6 and Table S4) and SEM images (Figure S7) of cured DGEBA, R-DGEBA and S-DGEBA also manifest that the disparate chirality in epoxy resins do not have the impact on the arrangement and the morphology of the molecular segments. This means chiral molecules of the same configuration will not be dissimilarly oriented in cured epoxy resin system. We suppose that there are several reasons for this. The major one is that DGEBA, R-DGEBA, and S-DGEBA have the same secondary structure. As shown in Figure 5(b), all the three epoxy resins have the positive cotton effect. It illustrates that the secondary structure of epoxy monomer is insusceptible to the chirality in epoxy group and the monomers of DGEBA, R-DGEBA, and S-DGEBA are all right helix structure. This imply that DGEBA, RDGEBA, and S-DGEBA have the equal structure in the cured three-dimensional polymer network, so there is no visible difference on the thermal stability, glass transition temperature, and thermomechanical properties. And it is also the possible reason that the covalent bonds connecting epoxy groups in 3D networks limits the orientation of chiral molecules and the curing agent (D230) molecules separated the epoxy monomer molecules and hindered their orientation.

3.4. Optical Activity of DGEBA, R-DGEBA, and S-DGEBA. It is difficult to obtain the optical activity of cured samples since the three-dimensional polymer network makes the epoxy resins inmeltable and insoluble. Therefore, the optical activity was achieved by the polarizer experiment and the results are shown in Figure 6. When the polarization directions of the two polarizations are completely same, according to Malus's Law, the optical path can pass normally, and the words BUCT marked on the rear polarizer can be observed (Figure 6(a)). While no light will pass through when the polarization directions are perpendicular, and thus "BUCT" cannot be seen (Figure 6(b)). However, the "BUCT" will be observed again via placing the transparent object with optical rotation between the two polarizations. Herein, we prepared the cured DGEBA, RDGEBA, and S-DGEBA that are all transparent (Figure 6(c)). Then the cured DGEBA, R-DGEBA, and S-DGEBA were set between the two polarizations film, respectively, as shown in Figure 6(d)–6(f). When the cured DGEBA was put between them, "BUCT" still can't be seen, while "BUCT" can be observed partly again when the cured R-DGEBA and the cured S-DGEBA were located between the two polarization films. These phenomena indicate that the chirality and optical activity are able to maintain, during the curing reaction process, because the chirality will be maintained during the curing of amines according to the curing mechanism (Scheme 3) including epoxy group reacting with primary and secondary amines, reactions catalyzed by tertiary amines and created hydroxyl groups.

The remarkable thing is that the chiral carbon will become pseudochiral carbon atom as the growth of molecular networks. Hence, only the chiral carbon atoms at the end of a polymer network can still exhibit the optical activity, and the cured products show only partial optical rotation.

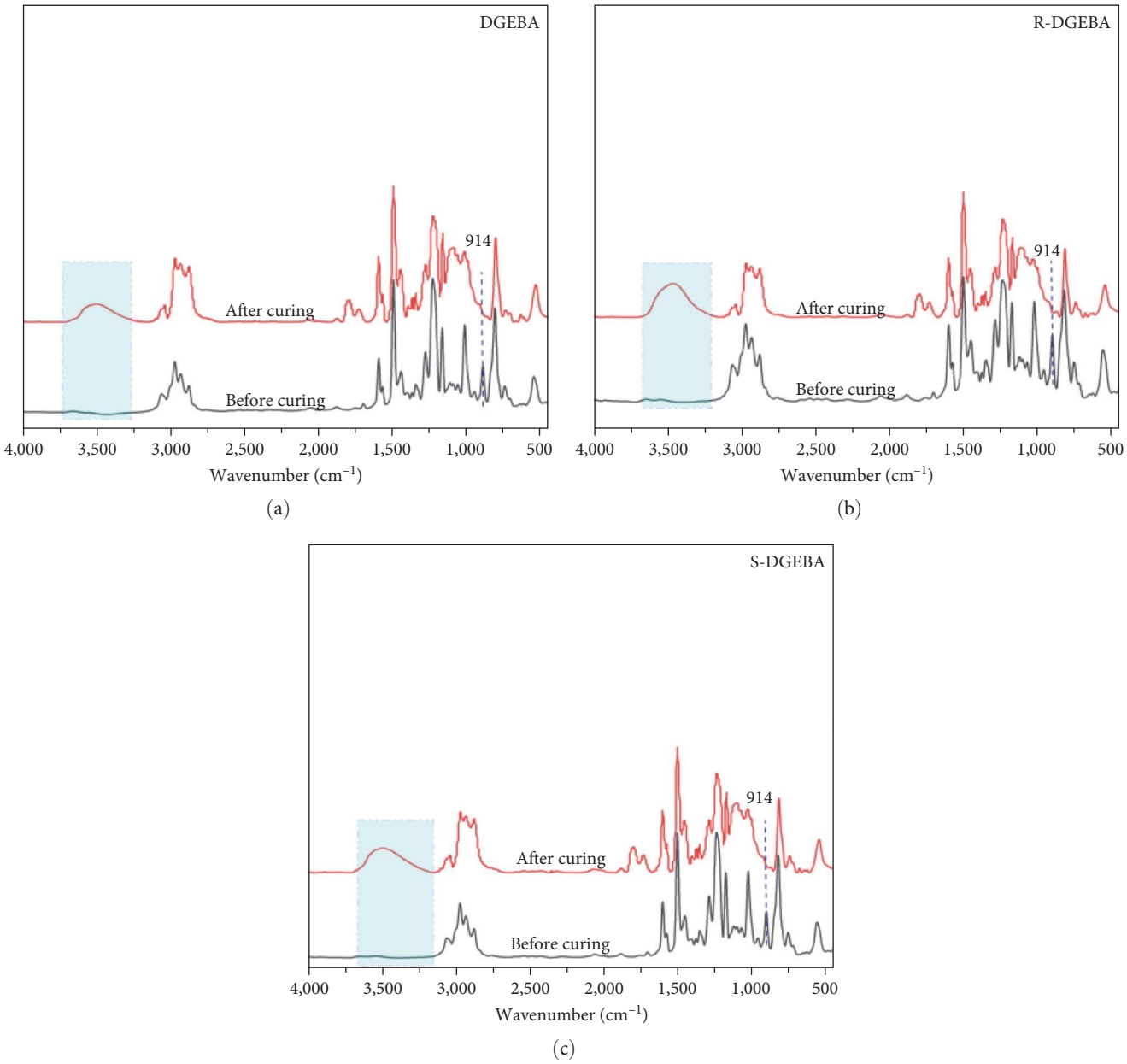

Figure 4: FTIR spectra of (a) DGEBA, (b) R-DGEBA, and (c) S-DGEBA before and after curing.

4. Conclusion

In this work, three epoxy resins named DGEBA, R-DGEBA, and S-DGEBA of different optical activity were prepared by one-pot reaction with ECH of diverse chiral configuration, respectively. This is simple preparation method for all the epoxy resins that can be acquired by the reaction with ECH. The chemical structure and chirality were confirmed by NMR, FTIR, HPLC, and optical rotation tester. For the first time, we investigated the curing process and cured properties of different chiral epoxy resins by using D230 as curing agent. The curing process E_as of DGEBA, R-DGEBA, and S-DGEBA with D230 are basically identical because of the epoxide ring-opening, during the curing course, occurring on achiral carbon of epoxy group. Thermal stability, glass transition temperature, and thermomechanical properties of the three cured samples were nearly same due to the alike three-dimensional polymer network caused by the same secondary right helix structure of the three epoxy monomers. Finally, on account of the chirality of carbon can be maintained in curing reaction, the cured products of the R-DGEBA and S-DGEBA exhibit the optical activity. But they can only show the partial optical activity owing to the many chiral carbons becoming pseudochiral carbon atom with the growth of molecular networks. This imply the cured products of chiral epoxy resins have a value on the field of polarized light materials. If chiral control is achieved through further research, we believe that this chiral epoxy resin will be as

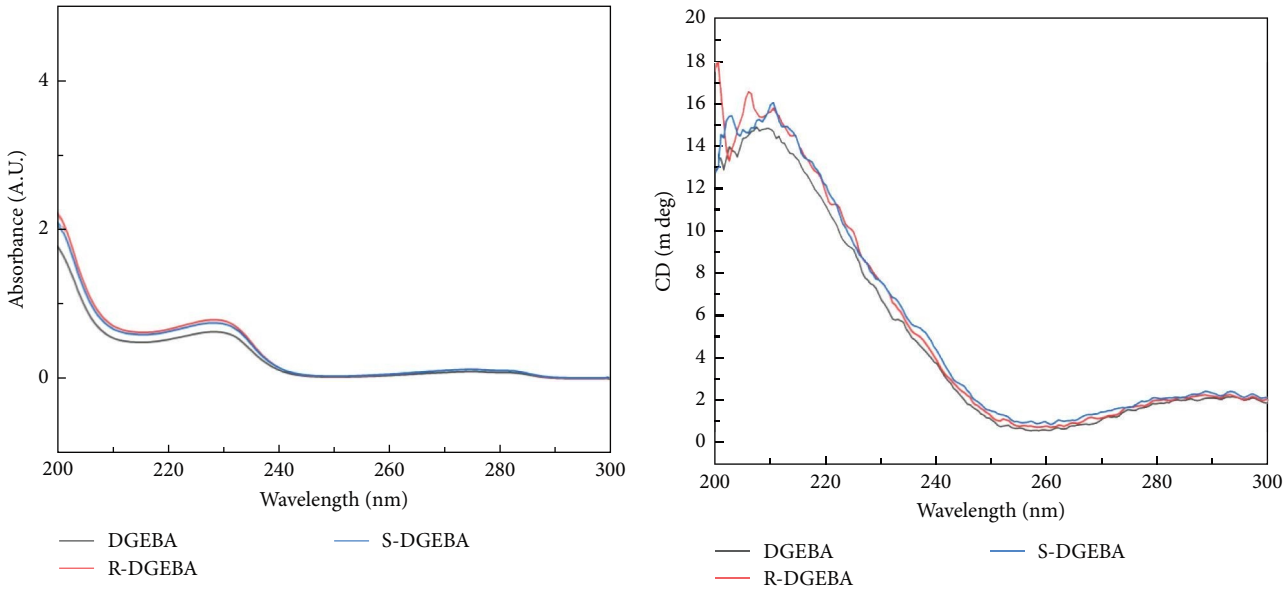

(a) (b)

FIGURE 5: UV and CD spectra of DGEBA, R-DGEBA, S-DGEBA: (a) UV spectra (0.1 mM in CH_3CN at room temperature); (b) CD spectra (0.05 mM in CH_3CN at room temperature).

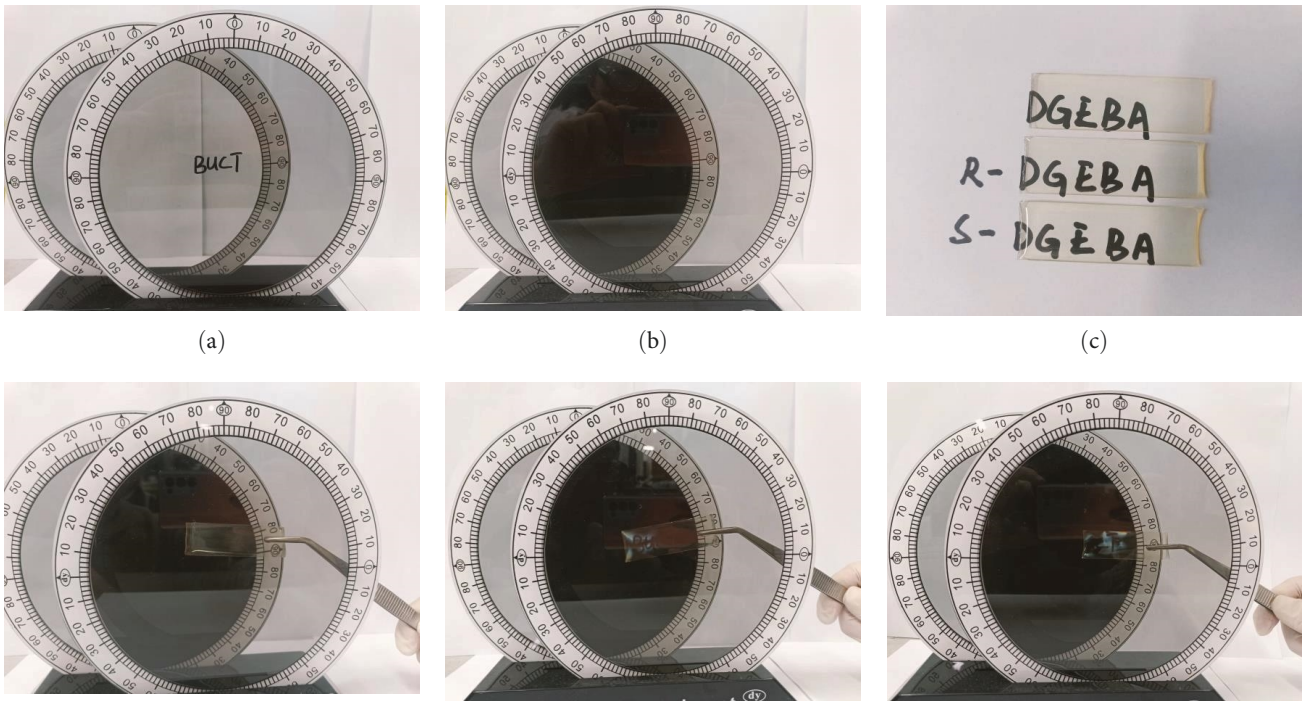

(a) (b) (c)

(d) (e) (f)

FIGURE 6: Observation of optical activity: (a) polarizations films with same polarization direction, (b) polarizations films with perpendicular polarization direction, (c) transparent cured epoxy resins, (d) DGEBA (e) R-DGEBA, and (f) S-DGEBA.

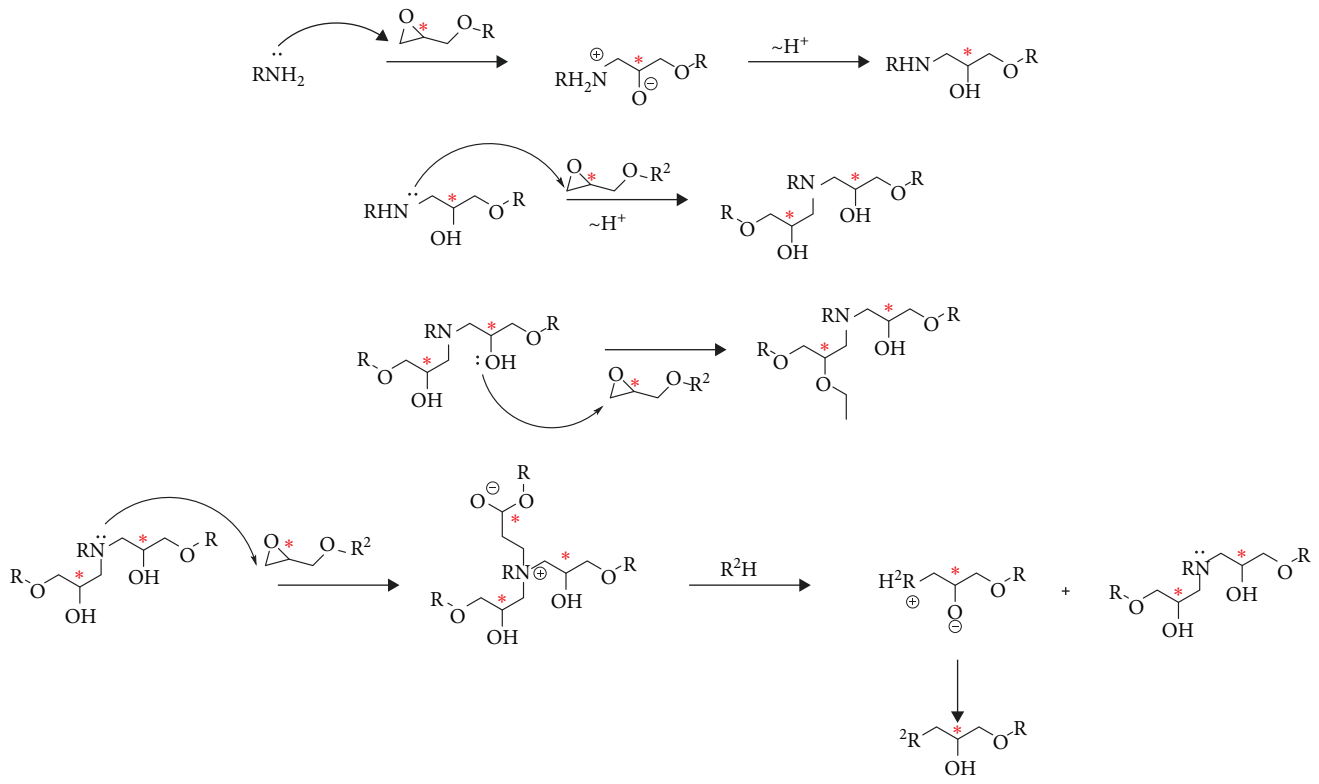

Scheme 3: Mechanisms in curing reaction of epoxy resin and D230.

important as other polarized light materials in 3D display, optical storage, optical anti-counterfeiting, and asymmetric synthesis.

Data Availability

The data used to support the findings of this study are included within the article and the supplementary information file(s).

Conflicts of Interest

The authors declare that they have no conflicts of interest.

Authors' Contributions

All the authors contributed equally to this work.

Acknowledgments

Thanks to each of the authors for their equal contributions to this article.

Supplementary Materials

Additional details contain the characterization of DGEBA, R-DGEBA, and S-DGEBA (^{13}C NMR spectra and MS data), and properties characterization involving DSC (including nonisothermal kinetics of curing reaction and T_g), TGA, DMA, XRD diagrams, and SEM images results of the cured DGEBA, R-DGEBA and S-DGEBA. Figure S1: ^{13}C NMR spectra. Figure S2: MS spectra. Figure S3: DSC tests at different heating rate. Figure S4: (a) TG and (b) DTG curves under a nitrogen atmosphere. Figure S5: results of cured DGEBA, R-DGEBA, and S-DGEBA of glass-transition temperature and DMA tests. Figure S6: XRD diagram of cured samples. Figure S7: SEM images of cured resins. Table S1: curing kinetic parameters. Table S2: TGA data of the cured epoxy resins. Table S3: data of DSC and DMA tests. Table S4: results of XRD tests. (*Supplementary Materials*)

References

[1] S. Utsunomiya, S. Sakamura, T. Sasamura et al., "Cells with broken left–right symmetry: roles of intrinsic cell chirality in left–right asymmetric epithelial morphogenesis," *Symmetry*, vol. 11, no. 4, Article ID 505, 2019.

[2] J. Jesús Pelayo, I. Valencia, A. Patricio García et al., "Chirality in bare and ligand-protected metal nanoclusters," *Advances in Physics: X*, vol. 3, no. 1, Article ID 1509727, 2018.

[3] J. R. Brandt, F. Salerno, and M. J. Fuchter, "The added value of small-molecule chirality in technological applications," *Nature Reviews Chemistry*, vol. 1, Article ID 0045, 2017.

[4] J. Budhathoki-Uprety and B. M. Novak, "Synthesis of alkyne-functionalized helical polycarbodiimides and their ligation to small molecules using 'click' and sonogashira reactions," *Macromolecules*, vol. 44, no. 15, pp. 5947–5954, 2011.

[5] J. F. Reuther, M. P. Bhatt, G. Tian, B. L. Batchelor, R. Campos, and B. M. Novak, "Controlled living polymerization of carbodiimides using versatile, air-stable nickel (II) initiators: facile incorporation of helical, rod-like materials," *Macromolecules*, vol. 47, no. 14, pp. 4587–4595, 2014.

[6] J. F. Reuther, D. A. Siriwardane, O. V. Kulikov, B. L. Batchelor, R. Campos, and B. M. Novak, "Facile synthesis of rod–coil

block copolymers with chiral, helical polycarbodiimide segments via postpolymerization CuAAC "click" coupling of functional end groups," *Macromolecules*, vol. 48, no. 10, pp. 3207–3216, 2015.

[7] J. F. Reuther, D. A. Siriwardane, R. Campos, and B. M. Novak, "Solvent tunable self-assembly of amphiphilic rod–coil block copolymers with chiral, helical polycarbodiimide segments: polymeric nanostructures with variable shapes and sizes," *Macromolecules*, vol. 48, no. 19, pp. 6890–6899, 2015.

[8] T. Yamamoto, T. Yamada, Y. Nagata, and M. Suginome, "High-molecular-weight polyquinoxaline-based helically chiral phosphine (PQXphos) as chirality-switchable, reusable, and highly enantioselective monodentate ligand in catalytic asymmetric hydrosilylation of styrenes," *Journal of the American Chemical Society*, vol. 132, no. 23, pp. 7899–901, 2010.

[9] S. J. George, Ž. Tomović, A. P. H. J. Schenning, and E. W. Meijer, "Insight into the chiral induction in supramolecular stacks through preferential chiral solvation," *Chemical Communications*, vol. 47, no. 12, pp. 3451–3453, 2011.

[10] H.-W. Chang, H.-I. Ma, Y.-S. Wu et al., "Site specific NMR characterization of abeta-40 oligomers cross seeded by abeta-42 oligomers," *Chemical Science*, vol. 13, no. 29, pp. 8526–8535, 2022.

[11] S. M. Katz, J. A. Reichl, and D. H. Berry, "Catalytic synthesis of poly(arylmethylgermanes) by demethanative coupling: a mild route to σ-conjugated polymers," *Journal of the American Chemical Society*, vol. 120, no. 38, pp. 9844–9849, 1998.

[12] A. Kadashchuk, Y. Skryshevski, A. Vakhnin et al., "Highly efficient intrinsic phosphorescence from a σ-conjugated poly(silylene) polymer," *The Journal of Physical Chemistry C*, vol. 118, no. 40, pp. 22923–22934, 2014.

[13] P. Puneet, R. Vedarajan, and N. Matsumi, "σ-p conjugated copolymers via dehydrocoupling polymerization of phenylsilane and mesitylborane," *Polymer Chemistry*, vol. 7, no. 25, pp. 4182–4187, 2016.

[14] S. Shinde, J. L. Sartucci, D. K. Jones, and N. Gavvalapalli, "Dynamic π-conjugated polymer ionic networks," *Macromolecules*, vol. 50, no. 19, pp. 7577–7583, 2017.

[15] G. E. J. Hicks, S. Li, N. K. Obhi, C. N. Jarrett-Wilkins, and D. S. Seferos, "Programmable assembly of π-conjugated polymers," *Advanced Materials*, vol. 33, no. 46, Article ID 2006287, 2021.

[16] T. Mikie and I. Osaka, "Small-bandgap quinoid-based π-conjugated polymers," *Journal of Materials Chemistry C*, vol. 8, no. 41, pp. 14262–14288, 2020.

[17] X. Zhang, M. Yu, and R. M. Laine, "An approach to epoxy resins: oxysilylation of epoxides," *Macromolecules*, vol. 53, no. 6, pp. 2249–2263, 2020.

[18] R. Auvergne, S. Caillol, G. David, B. Boutevin, and J.-P. Pascault, "Biobased thermosetting epoxy: present and future," *Chemical Reviews*, vol. 114, no. 2, pp. 1082–1115, 2014.

[19] C. Gioia, G. Lo Re, M. Lawoko, and L. Berglund, "Tunable thermosetting epoxies based on fractionated and well-characterized lignins," *Journal of the American Chemical Society*, vol. 140, no. 11, pp. 4054–4061, 2018.

[20] S. Wang, S. Ma, C. Xu et al., "Vanillin-derived high-performance flame retardant epoxy resins: facile synthesis and properties," *Macromolecules*, vol. 50, no. 5, pp. 1892–1901, 2017.

[21] X. Zhang, Q. He, H. Gu, H. A. Colorado, S. Wei, and Z. Guo, "Flame-retardant electrical conductive nanopolymers based on bisphenol F epoxy resin reinforced with nano polyanilines," *ACS Applied Materials & Interfaces*, vol. 5, no. 3, pp. 898–910, 2013.

[22] J. Zhu, S. Wei, J. Ryu, M. Budhathoki, G. Liang, and Z. Guo, "In situ stabilized carbon nanofiber (CNF) reinforced epoxy nanocomposites," *Journal of Materials Chemistry*, vol. 20, no. 23, pp. 4937–4948, 2010.

[23] X. Zhang, O. Alloul, Q. He et al., "Strengthened magnetic epoxy nanocomposites with protruding nanoparticles on the graphene nanosheets," *Polymer*, vol. 54, no. 14, pp. 3594–3604, 2013.

[24] N. Chand and A. Nigrawal, "Development and electrical conductivity behavior of copper-powder-filled-epoxy graded composites," *Journal of Applied Polymer Science*, vol. 109, no. 4, pp. 2384–2387, 2008.

[25] T.-H. Ho and C.-S. Wang, "Modification of epoxy resins with polysiloxane thermoplastic polyurethane for electronic encapsulation: 1," *Polymer*, vol. 37, no. 13, pp. 2733–2742, 1996.

[26] L.-L. Lin, T.-H. Ho, and C.-S. Wang, "Synthesis of novel trifunctional epoxy resins and their modification with polydimethylsiloxane for electronic application," *Polymer*, vol. 38, no. 8, pp. 1997–2003, 1997.

[27] H. Jin, C. L. Mangun, D. S. Stradley, J. S. Moore, N. R. Sottos, and S. R. White, "Self-healing thermoset using encapsulated epoxy-amine healing chemistry," *Polymer*, vol. 53, no. 2, pp. 581–587, 2012.

[28] H. Abdollahi, A. Ershad-Langroudi, A. Salimi, and A. Rahimi, "Anticorrosive coatings prepared using epoxy–silica hybrid nanocomposite materials," *Industrial & Engineering Chemistry Research*, vol. 53, no. 27, pp. 10858–10869, 2014.

[29] X. Shi, T. A. Nguyen, Z. Suo, Y. Liu, and R. Avci, "Effect of nanoparticles on the anticorrosion and mechanical properties of epoxy coating," *Surface and Coatings Technology*, vol. 204, no. 3, pp. 237–245, 2009.

[30] C. Acebo, X. Fernández-Francos, M. Messori, X. Ramis, and À. Serra, "Novel epoxy-silica hybrid coatings by using ethoxysilyl-modified hyperbranched poly(ethyleneimine) with improved scratch resistance," *Polymer*, vol. 55, no. 20, pp. 5028–5035, 2014.

[31] X.-L. Wang, Y.-Y. Yang, H.-J. Chen, Y. Wu, and D.-S. Ma, "Synthesis of a vinylchlorine-containing 1,3-diol from a marine cyanophyte," *Tetrahedron*, vol. 70, no. 30, pp. 4571–4579, 2014.

[32] F. Meng, L. Liu, W. Tian et al., "The influence of the chemically bonded interface between fillers and binder on the failure behaviour of an epoxy coating under marine alternating hydrostatic pressure," *Corrosion Science*, vol. 101, pp. 139–154, 2015.

[33] H. Gu, C. Ma, J. Gu et al., "An overview of multifunctional epoxy nanocomposites," *Journal of Materials Chemistry C*, vol. 4, no. 25, pp. 5890–5906, 2016.

[34] J. M. Klunder, S. Y. Ko, and K. B. Sharpless, "Asymmetric epoxidation of allyl alcohol: efficient routes to homochiral . beta.-adrenergic blocking agents," *The Journal of Organic Chemistry*, vol. 51, no. 19, pp. 3710–3712, 1986.

[35] Y. Gao, J. M. Klunder, R. M. Hanson, H. Masamune, S. Y. Ko, and K. B. Sharpless, "Catalytic asymmetric epoxidation and kinetic resolution: modified procedures including in situ derivatization," *Journal of the American Chemical Society*, vol. 109, no. 19, pp. 5765–5780, 1987.

[36] M. Breuer, K. Ditrich, T. Habicher et al., "Industrial methods for the production of optically active intermediates,"

Angewandte Chemie International Edition, vol. 43, no. 7, pp. 788–824, 2004.

[37] K. Wilson, "R. A. Sheldon, I. Arends and U. Hanefeld. Green chemistry and catalysis. Wiley-VCH, 2007, 448 Pp; ISBN 978-3-527-30715-9 (Hardcover)," *Applied Organometallic Chemistry*, vol. 21, no. 11, Article ID 1002, 2007.

[38] W. Zhang, J. L. Loebach, S. R. Wilson, and E. N. Jacobsen, "Enantioselective epoxidation of unfunctionalized olefins catalyzed by salen manganese complexes," *Journal of the American Chemical Society*, vol. 112, no. 7, pp. 2801–2803, 1990.

[39] L. Deng and E. N. Jacobsen, "A practical, highly enantioselective synthesis of the taxol side chain via asymmetric catalysis," *The Journal of Organic Chemistry*, vol. 57, no. 15, pp. 4320–4323, 1992.

[40] E. J. de Vries and D. B. Janssen, "Biocatalytic conversion of epoxides," *Current Opinion in Biotechnology*, vol. 14, no. 4, pp. 414–420, 2003.

[41] A. Steinreiber and K. Faber, "Microbial epoxide hydrolases for preparative biotransformations," *Current Opinion in Biotechnology*, vol. 12, no. 6, pp. 552–558, 2001.

[42] E. Y. Lee and M. L. Shuler, "Molecular engineering of epoxide hydrolase and its application to asymmetric and enantioconvergent hydrolysis," *Biotechnology and Bioengineering*, vol. 98, no. 2, pp. 318–327, 2007.

[43] A. Archelas and R. Furstoss, "Synthetic applications of epoxide hydrolases," *Current Opinion in Chemical Biology*, vol. 5, no. 2, pp. 112–119, 2001.

[44] S.-Q. Yang, A.-J. Han, Y. Liu, X.-Y. Tang, G.-Q. Lin, and Z.-T. He, "Catalytic asymmetric hydroalkoxylation and formal hydration and hydroaminoxylation of conjugated dienes," *Journal of the American Chemical Society*, vol. 145, no. 7, pp. 3915–3925, 2023.

[45] J.-M. Yang, Y.-K. Lin, T. Sheng, L. Hu, X.-P. Cai, and J.-Q. Yu, "Regio-controllable [2+2] benzannulation with two adjacent C (sp^3)–H bonds," *Science*, vol. 380, no. 6645, pp. 639–644, 2023.

[46] D. Roşu, C. N. Caşcaval, F. Mustąt , and C. Ciobanu, "Cure kinetics of epoxy resins studied by non-isothermal DSC data," *Thermochimica Acta*, vol. 383, no. 1-2, pp. 119–127, 2002.

[47] H. Cai, P. Li, G. Sui et al., "Curing kinetics study of epoxy resin/flexible amine toughness systems by dynamic and isothermal DSC," *Thermochimica Acta*, vol. 473, no. 1-2, pp. 101–105, 2008.

[48] C. S. Wang and C. H. Lin, "Properties and curing kinetic of diglycidyl ether of bisphenol a cured with a phosphorus-containing diamine," *Journal of Applied Polymer Science*, vol. 74, no. 7, pp. 1635–1645, 1999.

[49] A. Fernandez, C. Palacios, M. Echegaray, G. Mazza, and R. Rodriguez, "Pyrolysis and combustion of regional agro-industrial wastes: thermal behavior and kinetic parameters comparison," *Combustion Science and Technology*, vol. 190, no. 1, pp. 114–135, 2018.

[50] W. Miao, X. Li, Y. Wang, and Y. Lv, "Pyrolysis characteristics of oil-field sludge and the comparison of kinetic analysis with two representative methods," *Journal of Petroleum Science and Engineering*, vol. 182, Article ID 106309, 2019.